

Braiding of Atomic Majorana Fermions in Wire Networks and Implementation of the Deutsch-Josza Algorithm

Christina V. Kraus,^{1,2} P. Zoller,^{1,2} and Mikhail A. Baranov^{1,2,3}

¹*Institute for Quantum Optics and Quantum Information of the Austrian Academy of Sciences, A-6020 Innsbruck, Austria*

²*Institute for Theoretical Physics, Innsbruck University, A-6020 Innsbruck, Austria*

³*RRC "Kurchatov Institute", Kurchatov Square 1, 123182, Moscow, Russia*

We propose an efficient protocol for braiding atomic Majorana fermions in wire networks with AMO techniques and demonstrate its robustness against experimentally relevant errors. Based on this protocol we provide a topologically protected implementation of the Deutsch-Josza algorithm.

The prediction of particles with anyonic statistics in topological phases of matter has resulted in the proposal of decoherence-free Topological Quantum Computation (TQC) [1–3]. TQC requires the creation of anyonic particles as well as their controlled interchange, known as *braiding*, which is the fundamental building block of topological quantum gates [4, 5]. While the implementation of these tasks in real physical systems is an outstanding challenge, the reported observation of anyonic Majorana fermions (MFs) in hybrid superconductor-semiconductor nanowire devices [6–8] and the proposals for the manipulation [9–11] of anyonic Majorana fermions (MFs) in solid state systems are promising first steps in this direction [11–16]. A complementary and promising approach towards realizing and coherently control MFs are ultracold atoms confined to 1D optical lattices coupled to BCS or molecular atomic reservoirs. The recent realization of a quantum gas microscope [17, 18] for optical lattices adds single site addressing and measurement to the toolbox of possible atomic operations to create and detect MFs [19–21].

Building on these experimental advances, we describe in this Letter an efficient braiding protocol for atomic MFs, based on performing simple lattice operations on a few sites in an array of 1D wires, and we provide a careful study of the full braiding dynamics including imperfections. In addition, we will show that these elementary braiding operations, although they do not represent the complete set of quantum gates [22, 23], can be combined to realize a Deutsch-Josza algorithm [24], demonstrating that the implementation of simple quantum algorithms in atomic topological setups is within experimental reach.

Braiding of atomic Majorana fermions. We consider a system of single component fermions that are confined to an array of one-dimensional (1D) wires of L sites (see Fig. 1) and that are governed by a Hamiltonian $H = \sum_n H^{(n)}$. The Hamiltonian $H^{(n)} = \sum_{j=1}^{L-1} -J a_{n,j}^\dagger a_{n,j+1} + \Delta a_{n,j} a_{n,j+1} + h.c. - \mu \sum_n a_n^\dagger a_n$ realizes a Kitaev chain [25] in the n -th wire. The operators $a_{n,j}^\dagger$ and $a_{n,j}$ are fermionic creation and annihilation operators, $J > 0$ and $\Delta \in \mathbb{R}$ are nearest-neighbor hopping and pairing terms, and μ is a chemical potential. As demonstrated in [19], a Hamiltonian of the form $H^{(n)}$ allows for a cold atom implementation: While the hop-

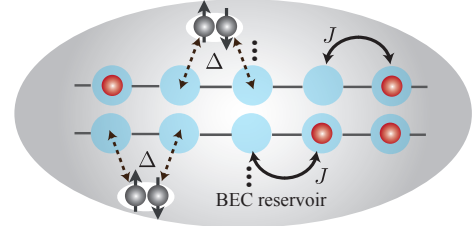


FIG. 1: Realization of an array of one-dimensional Kitaev wires in an optical lattice setup: Atoms (red circles) can hop between neighboring sites (blue circles) with strength J along the individual wires. The pairing term of strength Δ can be realized by a Raman induced dissociation of Cooper pairs (or Feshbach molecules) forming an atomic BCS reservoir.

ping term arises naturally in an optical lattice setup, the pairing term can be realized by a Raman induced dissociation of Cooper pairs (or Feshbach molecules) forming an atomic BCS reservoir.

It has been shown in [25] that the Hamiltonian $H^{(n)}$ supports zero energy Majorana fermions of the form $\gamma_{L/R}^{(n)} = \sum_j v_{n,j}^{L/R} c_{n,j}$ with (real) coefficients $v_{n,j}^{L/R}$ which are localized at the left/right end of the n -th wire. Here, $c_{n,2j-1} = a_{n,j}^\dagger + a_{n,j}$ and $c_{n,2j} = (-i)(a_{n,j}^\dagger - a_{n,j})$ are Majorana operators fulfilling $\{c_{n,k}, c_{m,l}\} = 2\delta_{kl}\delta_{mn}$. For the "ideal" quantum wire ($J = |\Delta|, \mu = 0$), one has $v_{n,1}^L = 1, v_{n,2L}^R = 1$ and else $v_{n,j}^{L/R} = 0$. Otherwise, the modes $\gamma_{L/R}^{(n)}$ decay exponentially inside the bulk. Each wire has two degenerate ground states $|0_n\rangle$ and $|1_n\rangle$ with even and odd parity, respectively, corresponding to the presence or absence of the Majorana fermion $f_n = \gamma_L^{(n)} - i\gamma_R^{(n)}$, i.e. $f_n|0_n\rangle = 0, f_n^\dagger|0_n\rangle = |1_n\rangle$. For a proposal how to prepare MFs in the desired parity subspace see [20].

Since MFs exhibit anyonic statistics, an appropriate interchange of two Majorana modes, $\gamma_{1,2}$, allows to realize the braiding unitary $U_b = e^{\pi\gamma_1\gamma_2/4}$. This interchange which leads to the transformation $\gamma_1 \mapsto -\gamma_2, \gamma_2 \mapsto \gamma_1$ resulting in a non-trivial phase factor for the wave function is the key step for realizing a TQC. In the following we present a protocol for a cold atom implementation that allows to realize braiding. To this end, we con-

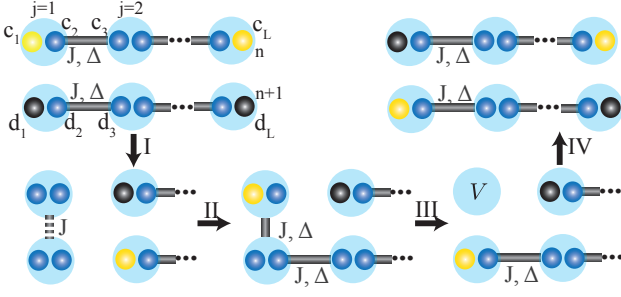


FIG. 2: Braiding protocol for two perfect quantum wires. The zero-energy Majorana modes that are initially on the upper (lower) wire are shown as yellow (black) spheres, while the blue ones corresponds to the Majorana operators which are coupled into finite-energy fermionic modes. Coupling of Majorana operators via hopping and pairing (Kitaev coupling) is indicated by grey solid links, while the coupling via hopping only is shown as a dashed link.

consider two neighboring wires n and $n+1$ governed by two ideal Kitaev Hamiltonians $H^{(n)}$ and $H^{(n+1)}$. The use of ideal wires allows for a simple analytic treatment because only six Majorana operators are involved in the protocol. It is convenient to label the sites by (w, j) , where $w = u, l$ denotes the upper (n) resp. lower ($n+1$) wire and $j = 1, \dots, L$. We label the sites that are involved in our protocol as $\vec{s}_1 = (u, 1)$, $\vec{s}_2 = (u, 2)$, $\vec{s}_3 = (l, 1)$ and $\vec{s}_4 = (l, 2)$ (see Fig. 2). To simplify notation, we write $c_{u,j} \equiv c_j$, and $c_{l,j} \equiv d_j$ with Majorana modes $\gamma_L^{(u)} = c_1$, $\gamma_R^{(u)} = c_L$, $\gamma_L^{(l)} = d_1$, $\gamma_R^{(l)} = d_L$.

Let us now show how to braid the left Majorana modes $\gamma_L^{(u)}$ and $\gamma_L^{(l)}$ around each other with only local (adiabatic) changes in the Hamiltonian on the left edge of the system. These changes include switching on/off (i) the hopping $H_{\vec{s}_i, \vec{s}_j}^{(h)} = -Ja_{\vec{s}_i}^\dagger a_{\vec{s}_j} + h.c.$ and (ii) the pairing $H_{\vec{s}_i, \vec{s}_j}^{(p)} = Ja_{\vec{s}_i} a_{\vec{s}_j} + h.c.$ between the neighboring sites \vec{s}_i and \vec{s}_j , and (iii) the local potential $H_{\vec{s}_i}^{(lp)} = 2Va_{\vec{s}_i}^\dagger a_{\vec{s}_i}$ on site \vec{s}_i . Note that a combination of (i) and (ii) allows to switch on/off the Kitaev coupling $H_{\vec{s}_i, \vec{s}_j}^{(K)} = H_{\vec{s}_i, \vec{s}_j}^{(h)} + H_{\vec{s}_i, \vec{s}_j}^{(p)}$. These operations are based on the single site/link addressing available in cold atom experiments [17, 26].

Let us now describe the braiding protocol in detail. The physical process behind is the transfer of one fermion from the system (i. e. either from the upper or from the lower wire) into the lower wire. We characterize the required adiabatic changes via a time-dependent parameter ϕ_t that varies from 0 to $\pi/2$, and perform them in four steps. In describing these steps, we will only write down the Hamiltonian for the four involved sites and follow the evolution of the zero modes which are always separated by a finite gap from the rest of the spectrum.

Step I: We decouple the two very left sites, \vec{s}_1 and \vec{s}_3 from the system by switching off the couplings $H_{\vec{s}_i, \vec{s}_j}^{(K)}$

between sites $\vec{s}_1 - \vec{s}_2$ and $\vec{s}_3 - \vec{s}_4$, and, at the same time, switch on the hopping between sites $\vec{s}_1 - \vec{s}_3$:

$$H_I(t) = \cos \phi_t (H_{\vec{s}_1 \vec{s}_2}^{(K)} + H_{\vec{s}_3 \vec{s}_4}^{(K)}) + \sin \phi_t H_{\vec{s}_1 \vec{s}_3}^{(h)} \\ = -iJ [\cos \phi_t (c_2 c_3 + d_2 d_3) + \sin \phi_t (c_2 d_1 - c_1 d_2)/2].$$

During this process the zero modes evolve according to $\gamma_L^{(u)}(\phi_t) = (2 \cos \phi_t c_1 - \sin \phi_t d_3)/\sqrt{1 + 3 \cos^2 \phi_t}$, $\gamma_L^{(l)}(\phi_t) = (2 \cos \phi_t d_1 - \sin \phi_t c_3)/\sqrt{1 + 3 \cos^2 \phi_t}$, such that at the end $\gamma_L^{(u)} = -d_3$ and $\gamma_L^{(l)} = -c_3$. Note that the two decoupled sites \vec{s}_1 and \vec{s}_3 carry exactly one fermion which has been taken out of the system.

Step II: We put now this fermion in the lower wire by switching on $H_{\vec{s}_i, \vec{s}_j}^{(K)}$ between sites $\vec{s}_3 - \vec{s}_4$, and $H_{\vec{s}_i, \vec{s}_j}^{(p)}$ between the sites $\vec{s}_1 - \vec{s}_3$:

$$H_{II}(t) = H_{\vec{s}_1 \vec{s}_3}^{(h)} + \sin \phi_t (H_{\vec{s}_1 \vec{s}_3}^{(p)} + H_{\vec{s}_3 \vec{s}_4}^{(K)}) = \\ -i\frac{J}{2} [(c_2 d_1 - c_1 d_2) + \sin \phi_t (c_2 d_1 + c_1 d_2 + 2d_2 d_3)].$$

The zero modes evolve as $\gamma_L^{(u)}(\phi_t) = (2 \sin \phi_t c_1 - (1 - \sin \phi_t) d_3)/\sqrt{4 \sin^2 \phi_t + (1 - \sin \phi_t)^2}$, $\gamma_L^{(l)} = -c_3$, such that at the end $\gamma_L^{(u)} = c_1$ and $\gamma_L^{(l)} = -c_3$. Note, that at this stage the Majorana mode $\gamma_L^{(u)}$ ($\gamma_L^{(l)}$) has already been moved from the upper (lower) to the lower (upper) wire. However, two additional steps are needed to recover the original configuration of the wires.

Step III: We move the Majorana mode from the site \vec{s}_1 to the site \vec{s}_3 by switching on $H_{\vec{s}_1}^{(lp)}$ and simultaneously switching off $H_{\vec{s}_i, \vec{s}_j}^{(K)}$ between the sites $\vec{s}_1 - \vec{s}_3$:

$$H_{III}(t) = \sin \phi_t H_{\vec{s}_1}^{(lp)} + \cos \phi_t H_{\vec{s}_1 \vec{s}_3}^{(K)} + H_{\vec{s}_3 \vec{s}_4}^{(K)} \\ = -iJ (c_2 d_1 \cos \phi_t + d_2 d_3) - iV \sin \phi_t c_1 c_2.$$

The evolution of the zero mode $\gamma_L^{(u)} = (J \cos \phi_t c_1 + V \sin \phi_t d_1)/\sqrt{(J \cos \phi_t)^2 + (V \sin \phi_t)^2}$ results in $\gamma_L^{(u)} = d_1$, while $\gamma_L^{(l)} = -c_3$ remains fixed.

Step IV: Finally, we switch off $H_{\vec{s}_1}^{(lp)}$ and switch on $H_{\vec{s}_1 \vec{s}_2}^{(K)}$:

$$H_{IV}(t) = \sin \phi_t H_{\vec{s}_1 \vec{s}_2}^{(K)} + H_{\vec{s}_3 \vec{s}_4}^{(K)} + \cos \phi_t H_{\vec{s}_1}^{(lp)} \\ = -iJ [\sin \phi_t c_2 c_3 + d_2 d_3] - iV \cos \phi_t c_1 c_2$$

The zero modes are given by $\gamma_L^{(u)} = d_1$, $\gamma_L^{(l)} = -(J \sin \phi_t c_1 + V \cos \phi_t c_3)/\sqrt{(J \sin \phi_t)^2 + (V \cos \phi_t)^2}$, so that finally we get the desired braiding $\gamma_L^{(u)} \mapsto \gamma_L^{(l)}$ and $\gamma_L^{(l)} \mapsto -\gamma_L^{(u)}$ of left the Majorana modes on the wires n and $n+1$, which corresponds (up to unimportant phase factor) to the unitary $U_n = e^{\pi \gamma_L^{(u)} \gamma_L^{(l)}/4}$.

Note that the braiding in the other direction, U_n^\dagger and $\gamma_L^{(u)} \mapsto -\gamma_L^{(l)}$, $\gamma_L^{(l)} \mapsto \gamma_L^{(u)}$, can be achieved by putting the uncoupled fermion in the upper (instead of the lower) wire with a simple modification of Steps II-IV.

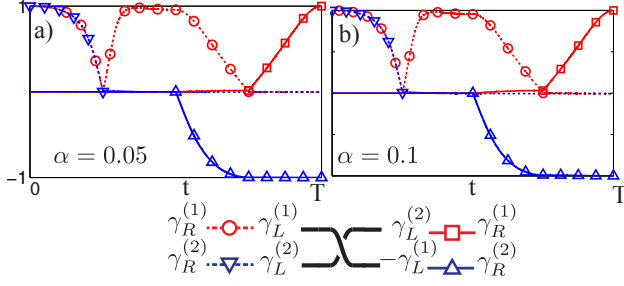


FIG. 3: Evolution of the Majorana correlation functions $\langle i\gamma_L^{(1)}\gamma_R^{(1)} \rangle$ (red, \circ), $\langle i\gamma_L^{(2)}\gamma_R^{(2)} \rangle$ (blue, ∇), $\langle i\gamma_L^{(2)}\gamma_R^{(1)} \rangle$ (red, \square), and $\langle i\gamma_L^{(1)}\gamma_R^{(2)} \rangle$ (blue, \triangle) during the braiding protocol with errors α in the local operations for two non-ideal quantum wires with $|\Delta| = 1.5J$ and $\mu = 0$. Markers are only drawn in regions where the correlation functions are non-zero.

The braiding results in the change of the correlation functions of the Majorana operators (see Fig. 2) and thus changes also the long-range fermionic correlations. This can also be translated into the change of the fermionic parities of the wires: If $|0_n\rangle$ ($|1_n\rangle$) denotes the state of the n -th wire with even (odd) parity and, for example, we start from the state $|0_n0_{n+1}\rangle$ with both wires with even parity, then the braiding U_n results in $U_n|0_n0_{n+1}\rangle = (|0_n0_{n+1}\rangle + |1_n1_{n+1}\rangle)/\sqrt{2}$, and $U_n^2|0_n0_{n+1}\rangle = |1_n1_{n+1}\rangle$. The result of the braiding, therefore, can be checked by measuring the change of the Majorana correlation functions in Time-of-Flight or spectroscopic experiments [20], or by measuring the parity of the wires by counting the number of fermions modulo two [18].

Non-ideal wires and non-perfect operations. We have just demonstrated the braiding for the case of ideal Kitaev wires and perfect local operations (single site/link addressing). Remarkably, the topological origin of the Majorana modes ensures the robustness of the results of the braiding protocol based on Steps I-IV also in the realistic case of non-ideal wires and local operations provided the Majorana modes are spatially well-separated. We have checked this numerically by considering two non-ideal wires with $J \neq |\Delta|$, $\mu \neq 0$ and assuming that the local operations have an error α in the following sense: (i) Switching on the hopping J and/or the pairing Δ between the sites $(u, 1) - (d, 1)$, also introduces the hopping $J\alpha$ and/or the pairing $\alpha\Delta$ between the adjacent sites $(u, 2) - (d, 2)$. (ii) Switching off the couplings between the sites $(w, 1) - (w, 2)$ also reduces the couplings between the sites $(w, 2) - (w, 3)$ by a factor $(1 - \alpha)$. (iii) Raising the local potential V on the site $(u, 1)$ results in a local potential αV on the neighboring sites $(u, 2)$ and $(l, 1)$. As an example, we present in Fig. 3 numerical results of the braiding protocol with errors $\alpha = 0.05$ and $\alpha = 0.1$ in the local operations for two quantum wires of the length $L = 40$ with $|\Delta| = 1.5J$ and $\mu = 0$. One can clearly see the robustness of the final results of the

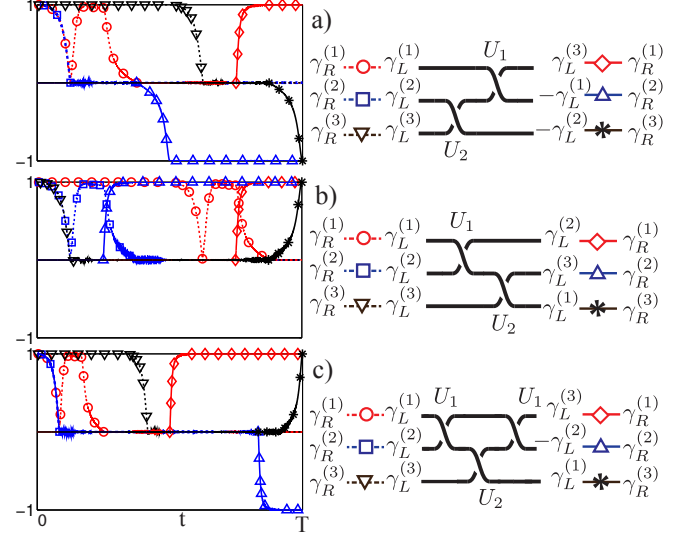


FIG. 4: Braid group in a setup of three wires. We present the real-time evolution of the correlations functions $i\langle \gamma_L^{(n)}\gamma_R^{(m)} \rangle$ under the action of (a) U_2U_1 , (b) U_1U_2 and (c) $U_1U_2U_1$ for a chain of the length $L = 40$ with $|\Delta| = 1.5J$ and $\mu = 0$. Markers are only drawn in regions where the correlation functions are non-zero.

braiding.

Braid group. It is also easy to check that the unitary transformations U_n of the Majorana operators corresponding to the braiding protocol fulfill all necessary conditions of the braid group [2]: For any two braiding unitaries U_n and U_{n+1} , one has $U_nU_{n+1} \neq U_{n+1}U_n$ and $U_{n-1}U_nU_{n-1} = U_nU_{n-1}U_n$.

To demonstrate this, consider three wires with left Majorana modes $\gamma_L^{(1)}$, $\gamma_L^{(2)}$ and $\gamma_L^{(3)}$, and braiding unitaries $U_1 = e^{\pi\gamma_L^{(1)}\gamma_L^{(2)}/4}$ and $U_2 = e^{\pi\gamma_L^{(2)}\gamma_L^{(3)}/4}$ that braid the modes $\gamma_L^{(1)}$, $\gamma_L^{(2)}$ and $\gamma_L^{(2)}$, $\gamma_L^{(3)}$, respectively. The braid group conditions for U_1 and U_2 then immediately follow from the following formulae

$$\begin{aligned} U_1U_2(\gamma_L^{(1)}, \gamma_L^{(2)}, \gamma_L^{(3)}) &= (\gamma_L^{(3)}, -\gamma_L^{(1)}, -\gamma_L^{(2)}) \\ U_2U_1(\gamma_L^{(1)}, \gamma_L^{(2)}, \gamma_L^{(3)}) &= (\gamma_L^{(2)}, \gamma_L^{(3)}, \gamma_L^{(1)}) \\ U_1U_2U_1(\gamma_L^{(1)}, \gamma_L^{(2)}, \gamma_L^{(3)}) &= (\gamma_L^{(3)}, -\gamma_L^{(2)}, \gamma_L^{(1)}) = \\ U_2U_1U_2(\gamma_L^{(1)}, \gamma_L^{(2)}, \gamma_L^{(3)}) &. \end{aligned} \quad (1) \quad (2)$$

These properties can be tested experimentally by measuring the corresponding changes of the fermionic correlation functions. For example, the action of U_1U_2 results in $i\langle \gamma_L^{(1)}\gamma_R^{(1)} \rangle \mapsto i\langle \gamma_L^{(3)}\gamma_R^{(1)} \rangle$, $i\langle \gamma_L^{(2)}\gamma_R^{(2)} \rangle \mapsto -i\langle \gamma_L^{(1)}\gamma_R^{(2)} \rangle$ and $i\langle \gamma_L^{(3)}\gamma_R^{(3)} \rangle \mapsto -i\langle \gamma_L^{(2)}\gamma_R^{(3)} \rangle$, while $U_1U_2U_1$ produces the following changes: $i\langle \gamma_L^{(1)}\gamma_R^{(1)} \rangle \mapsto i\langle \gamma_L^{(3)}\gamma_R^{(1)} \rangle$, $i\langle \gamma_L^{(2)}\gamma_R^{(2)} \rangle \mapsto -i\langle \gamma_L^{(2)}\gamma_R^{(1)} \rangle$, and $i\langle \gamma_L^{(3)}\gamma_R^{(3)} \rangle \mapsto i\langle \gamma_L^{(1)}\gamma_R^{(3)} \rangle$ (see Fig. 4). This change in the correlation functions can be measured, for example, in TOF or spectroscopic experiments as proposed in Ref. [20].

Deutsch-Josza algorithm. Although the braiding of MFs is robust, it does not provide a tool to construct a universal set of gates needed for TQC: As it has been shown in Ref. [23], only a subgroup of the Clifford group can be realized via braiding. Fortunately, not all QC algorithms require a universal set of gates. One example is the Deutsch-Josza algorithm [24] which, as we will show below, can be implemented for two qubits in a remarkably efficient way via braiding of MFs.

The Deutsch-Josza algorithm allows to determine whether the function ("oracle") $g(x)$ which is defined on the space of states of n qubits and takes the values 0 or 1, $g : \{|0\rangle, |1\rangle\}^{\otimes n} \mapsto \{0, 1\}$, is constant (has the same value, say, 0, for all inputs) or balanced (takes value 0 for half of the inputs, and 1 for the other half). For the algorithm to work, the function g has to be implemented as the unitary $U_g : |x\rangle \mapsto (-1)^{g(x)}|x\rangle$, where $|x\rangle \in \{|0\rangle, |1\rangle\}^{\otimes n}$, which is actually a major problem for experimental realizations: A faulty oracle spoils the quantum speedup [27].

For two qubits with the computational basis $\{|00\rangle, |01\rangle, |10\rangle, |11\rangle\}$, a possible choice for U_g is

$$U_{g_0} = \text{diag}(1, 1, 1, 1), \quad U_{g_1} = \text{diag}(1, 1, -1, -1), \\ U_{g_2} = \text{diag}(1, -1, -1, 1), \quad U_{g_3} = \text{diag}(1, -1, 1, -1),$$

for the constant g_0 and the balanced g_1, g_2 , and g_3 oracle functions, respectively. (Note that an equivalent set of oracles can be obtained by multiplying the above unitaries with -1 .) The algorithm works then in the following way: After preparing the system in the state $|00\rangle$, we apply the Hadamard gate H to each qubit, $H|0\rangle = (|0\rangle + |1\rangle)/\sqrt{2}$, $H|1\rangle = (|0\rangle - |1\rangle)/\sqrt{2}$, then we apply the unitary U_g corresponding to the oracle under test, then again the Hadamard gate to each qubit, and, finally, we measure the probability to find the system in the state $|00\rangle$. This probability is 1 if $g(x)$ is constant, and 0 if $g(x)$ is balanced, as can be seen from the following calculations

$$|00\rangle \xrightarrow{H \otimes H} \frac{1}{2} \sum_{\mathbf{x}} |\mathbf{x}\rangle \xrightarrow{U_g} \frac{1}{2} \sum_{\mathbf{x}} (-1)^{g(\mathbf{x})} |\mathbf{x}\rangle \\ \xrightarrow{H \otimes H} \frac{1}{4} \sum_{\mathbf{x}} (-1)^{g(\mathbf{x})} \sum_{\mathbf{y}} (-1)^{\mathbf{x} \cdot \mathbf{y}} |\mathbf{y}\rangle, \quad (3)$$

where we define $\mathbf{x} = (x_1, x_2)$ and $\mathbf{y} = (y_1, y_2)$ with $x_i, y_i \in \{0, 1\}$, and $\mathbf{x} \cdot \mathbf{y} = x_1 y_1 + x_2 y_2$.

To implement the above algorithm, we use a setup of three quantum wires in the geometry shown in Fig. 5 and define a computational basis for two qubits as $|00\rangle = f_2^\dagger |0_f\rangle$, $|01\rangle = f_3^\dagger |0_f\rangle$, $|10\rangle = f_1^\dagger |0_f\rangle$, and $|11\rangle = f_1^\dagger f_2^\dagger f_3^\dagger |0_f\rangle$ [22]. Here $|0_f\rangle$ is the vacuum state for fermionic modes $f_i = (\gamma_i^{(L)} - i\gamma_i^{(R)})/2$, where $\gamma_i^{(L)}$ and $\gamma_i^{(R)}$ are two Majorana modes on the i -th wire. Note that in this setup with three wires we encode only

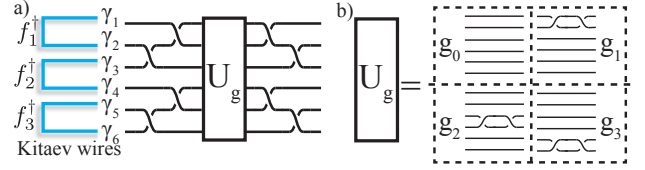


FIG. 5: a) Setup and implementation of the "oracle" Deutsch-Josza algorithm for two qubits via braiding. b) Implementation of the "oracle" unitary U_g via braiding (see main text).

two qubits [28]. This is because the braiding preserves fermionic parity and, therefore, all states from the computational basis must have the same parity (odd in our case).

The Hadamard gates and the oracle unitaries U_{g_i} can be implemented by noting that the braiding of Majorana modes γ_i and γ_j is equivalent to the unitary $U_{ij} = e^{\pi \gamma_i \gamma_j / 4} = (\mathbb{1} - \gamma_i \gamma_j) / \sqrt{2}$. Then, it follows immediately that $H \otimes \mathbb{1} = U_{12} U_{23} U_{12}$ and $\mathbb{1} \otimes H = U_{56} U_{45} U_{56}$ for the Hadamard gates acting on the first and the second qubit, respectively, and $U_{g_1} = U_{12}^2$, $U_{g_2} = U_{34}^2$, and $U_{g_3} = U_{56}^2$ for the oracle unitaries ($U_{g_0} = \mathbb{1}$). As a result, the Deutsch-Josza algorithm can be realized with 14 braiding operations. In our case, however, the number of operations can be reduced to nine: The sequence

$$\mathcal{U}_i = U_{45} U_{56} U_{23} U_{12} U_{g_i} U_{56} U_{45} U_{12} U_{23}$$

acting on $|00\rangle$ gives $\mathcal{U}_0|00\rangle = |00\rangle$ for the constant case and $\mathcal{U}_1|00\rangle = i|10\rangle$, $\mathcal{U}_2|00\rangle = |11\rangle$, and $\mathcal{U}_3|00\rangle = i|01\rangle$ for the balanced case. Note also that this protocol can be implemented in five steps because operations on the Majorana modes $\gamma_{1,2,3}$ and $\gamma_{4,5,6}$ before and after the oracle unitary U_{g_i} can be performed in parallel. The final state of the system and, therefore, the probability to find it in the state $|00\rangle$, can be determined by measuring the parities of the individual wires in a spectroscopic experiment [20] or fermionic number counting [18]. Taking into account the discussed insensitivity of the braiding to experimental imperfections, the proposed protocol provides a robust implementation of the Deutsch-Josza algorithm.

Conclusion. We have presented an efficient way of braiding MFs in a cold-atom setup and used it to implement the Deutsch-Josza algorithm in a topologically protected way. By adding well-controlled though topologically unprotected operations (e.g. the SWAP-gate), one can go beyond the braid group and provide a universal "hybrid" set of gates for quantum computation (see also Ref. [29, 30]). We address this issue in our future work.

Acknowledgments. We thank I. Bloch, F. Gerbier, N. Goldman, C. Gross, C. Laflamme, S. Nascimbène and N. Yao for useful comments and discussions. This work has been supported by the Austrian Science Fund FWF (SFB FOQUS F4015-N16), the US Army Research Office with

funding from the DARPA OLE program and the European Commission via the integrated project AQUITE.

-
- [1] A Kitaev. *Ann. Phys.*, 303:230, 2003.
 - [2] C. Nayak, Steven H. Simon, A. Stern, M. Freedman, and S. Das Sarma. *Rev. Mod. Phys.*, 80:1083–1159, 2008.
 - [3] J.K. Pachos, *Introduction to Topological Quantum Computation*, (Cambridge University Press, Cambridge, 2012)
 - [4] S. Das Sarma, M. Freedman, and C. Nayak. *Phys. Rev. Lett.*, 94:166802, 2005.
 - [5] C. Zhang, V.W. Scarola, S. Tewari, and S. Das Sarma. *Proc. Natl. Acad. Sci. USA*, 104:18415, 2007.
 - [6] V. Mourik, K Zuo, S. M. Frolov, S. R. Plissard, E. P. A. M Bakkers, and L. P Kouwenhoven. *Science*, 336:1003, 2012.
 - [7] M. T Deng, C .L Yu, G.Y Huang, M. Larson, P. Caroff, and H.Q. Xu. *Nano Lett.*, 12:6416, 2012.
 - [8] A. Das, Y. Ronen, Y. Most, Y. Oreg, M. Heiblum, and H. Shtrikman. *Nat. Phys.*, 8:887, 2012.
 - [9] J. Alicea, Y. Oreg, G. Refael, F. von Oppen, and M. P. A. Fisher. *Nat. Phys.*, 7:412, 2011.
 - [10] B. I. Halperin, Y. Oreg, A. Stern, G. Refael, J. Alicea, and F. von Oppen. *Phys. Rev. B*, 85:144501, 2012.
 - [11] M. Burrello, B. van Heck, and A. R. Akhmerov. *arXiv:1210.5452*, 2012.
 - [12] C. W. J. Beenakker. *arXiv:1112.1950*, 2011.
 - [13] F. Hassler, A. R. Akhmerov, C.-Y. Hou, and C. W. J. Beenakker. *New J. Phys.*, 12:125002, 2010.
 - [14] K. Flensberg. *Phys. Rev. Lett.*, 106:090503, 2011.
 - [15] M. Leijnse and K. Flensberg. *Phys. Rev. B*, 86:104511, 2012.
 - [16] D. Pekker, C.-Y. Hou, V. Manucharyan, and E. Demler. *arXiv:1301.3161*, 2013.
 - [17] J. Simon, W. S. Bakr, R. Ma, M. E. Tai, P. M. Preiss, and M. Greiner. *Nature (London)*, 472:307–312, 2011.
 - [18] J. F. Sherson, C. Weitenberg, M. Endres, M. Cheneau, I. Bloch, and S. Kuhr. *Nature (London)*, 467:68–72, 2010.
 - [19] L. Jiang, T. Kitagawa, J. Alicea, A. R. Akhmerov, D. Pekker, G. Refael, J. I. Cirac, E. Demler, M. D. Lukin, and P. Zoller. *Phys. Rev. Lett.*, 106:220402, 2011.
 - [20] C. V. Kraus, S. Diehl, M. A. Baranov, and P. Zoller. *New J. Phys.*, 14:113036, 2012.
 - [21] S. Nascimbène. *ArXiv e-prints*, 2012.
 - [22] C. Nayak and F. Wilczek. *Nucl. Phys. B*, 479:529, 1996.
 - [23] A. Ahlbrecht, L. S. Georgiev, and R. F. Werner. *Phys. Rev. A*, 79:032311, 2009.
 - [24] D. Deutsch and R. Jozsa. *Proceedings of the Royal Society of London, Series A*, 439:553, 1992.
 - [25] A. Y. Kitaev. *Physics-Uspekhi*, 44(10S):131, 2001.
 - [26] C. Weitenberg, M. Endres, J. F. Sherson, M. Cheneau, P. Schauß, T. Fukuhara, I. Bloch, and S. Kuhr. *Nature (London)*, 471:319–324, 2011.
 - [27] O. Regev and L. Schiff. *Proc. of ICALP*, 2008.
 - [28] L. S. Georgiev. *Phys. Rev. B*, 74:235112, 2006.
 - [29] D. J. Clarke, J. D. Sau, and S. Tewari. *Phys. Rev. B*, 84:035120, 2011.
 - [30] J. D. Sau, S. Tewari, and S. Das Sarma. *Phys. Rev. A*, 82:052322, 2010.